Table 1. Crystallographic statistics. GlpF was overexpressed, purified, and crystallized as described (6), replacing glycerol by xylose (15% w/w) for (GlpF-G)$_A$ and (GlpF-G)$_B$, a nontransported substrate (6). Single crystals were subject to x-ray diffraction at ALS beam line 5.0.2 using a CCD detector (Quantum IV). The crystals were in space group I422 and were isomorphous to crystals previously grown in 15% (w/w) glycerol. The structures were determined by direct isomorphous replacement using the protein component of 1FX8 and refined with CNS (27). The RMSD between 1FX8 (at 2.2 Å resolution) and (GlpF-G)$_A$ is 0.26 Å, and (GlpF-G)$_B$ is 0.51 Å and GlpF$^{W48F/F200T}$ is 0.20 Å, the RMSD between (GlpF-G)$_A$ and (GlpF-G)$_B$ is 0.18 Å.

Crystal	(GlpF-G)$_A$	(GlpF-G)$_B$	GlpF$^{W48F/F200T}$
Wavelength (Å)	1.1	1.1	1.0
Resolution (Å)	30−2.7	30−2.8	35−2.1
Observations	64951	51474	128187
Unique	10918	8698	25710
Unit cell size (a, c in Å)	96.05, 184.20	96.23, 184.37	96.93, 185.43
Completeness (%)	87.5	78.6	97.9
R_{merge} (%)	8.1	9.0	8.5
$\langle I/\sigma I \rangle$	14.0	16.9	16.0
Refinement statistics			
Number of reflections	9774/1144	7769/929	25674/1240
Number of nonhydrogen atoms	1997	1997	1994
Unobserved residues	1-5, 260−281	1-5, 260−281	1-5, 260−281
Resolution (Å)	30−2.7	30−2.8	35−2.1
R_{cryst}/R_{free} (%)	22.9/26.1	20.8/24.9	23.0/24.3
Average B factor (Å²)	54.4	49.6	40.3
Model geometry			
Bond length deviation (Å)	0.007	0.009	0.0063
Bond angle deviation (°)	1.26	1.11	1.17

$\langle I/\sigma I \rangle$, mean signal-to-noise, where I is the integrated intensity of a measured reflection and σI is the estimated error in the measurement; $R_{merge} = \Sigma_{hkl}\Sigma_i |I_i (hkl) − \langle I_i (hkl) \rangle | / \Sigma_{hkl}\Sigma_i I_i(hkl)$.

W48F/F200T double mutant, we started from the equilibrated model of the native protein in the membrane. After mutating the amino acids, the system was equilibrated (1 ns), followed by a 4 ns simulation used in our analysis. Simulation conditions were the same as for wild-type GlpF.

15. Supplementary materials are available at www.sciencemag.org/cgi/content/full/296/5567/525/DC1.
16. J. B. Heymann, A. Engel, *News Physiol. Sci.* **14**, 187 (1999).
17. M. J. Borgnia, D. Kozono, G. Calamita, P. C. Maloney, P. Agre, *J. Mol. Biol.* **291**, 1169 (1999).
18. M. J. Borgnia, P. Agre, *Proc. Natl. Acad. Sci. U.S.A.* **98**, 2888 (2001).
19. B. L. de Groot, H. Grubmüller, *Science* **294**, 2353 (2001).
20. I. V. Kurinov, R. W. Harrison, *Acta Crystallogr. D* **51**, 98 (1995).
21. D. Vitkup, D. Ringe, G. A. Petsko, M. Karplus, *Nature Struct. Biol.* **7**, 34 (2000).
22. J. P. Cowin, A. A. Tsekouras, M. J. Ledema, K. Wu, G. B. Ellison, *Nature* **398**, 405 (1999).
23. K. Murata *et al.*, *Nature* **407**, 599 (2000).
24. L. Kale *et al.*, *J. Comput. Phys.* **151**, 283 (1999).
25. A. D. MacKerell Jr. *et al.*, *J. Phys. Chem. B* **102**, 3586 (1998).
26. W. L. Jorgensen, J. Chandrasekhar, J. D. Madura, R. W. Impey, M. L. Klein, *J. Chem. Phys.* **79**, 926 (1983).
27. A. Brünger *et al.*, CNS program (1996).
28. O. Smart, Hole2 program (http://bach.bip.bham.ac.uk/osmart/hole/).
29. W. Humphrey, A. Dalke, K. Schulten, *J. Mol. Graph.* **14**, 33 (1996).
30. Supported by NIH, and computer time provided by NRAC. E.T. and P.N. received postdoctoral support from the Human Frontier Science Program Organization. M.Ø.J. acknowledges financial support from The Danish Natural Science Research Council. We thank E. Hur and W. Harries for constructing mutants, and T. Earnest for help and support at the Advanced Light Source (ALS), Lawrence Berkeley National Laboratory. Coordinates of the structures have been deposited in the Research Collaboratory for Structural Bioinformatics (RCSB) Protein Data Bank [accession codes 1LDI, 1LDA, and 1LDF for (GlpF-G)$_A$, (GlpF-G)$_B$, and GlpF$^{(W48F/F200T}$, respectively].

6 November 2001; accepted 14 March 2002

DNA Repair Pathway Stimulated by the Forkhead Transcription Factor FOXO3a Through the Gadd45 Protein

Hien Tran,[1]* Anne Brunet,[1]* Jill M. Grenier,[2] Sandeep R. Datta,[1] Albert J. Fornace Jr.,[3] Peter S. DiStefano,[2] Lillian W. Chiang,[2] Michael E. Greenberg[1]†

The signaling pathway from phosphoinositide 3-kinase to the protein kinase Akt controls organismal life-span in invertebrates and cell survival and proliferation in mammals by inhibiting the activity of members of the FOXO family of transcription factors. We show that mammalian FOXO3a also functions at the G$_2$ to M checkpoint in the cell cycle and triggers the repair of damaged DNA. By gene array analysis, FOXO3a was found to modulate the expression of several genes that regulate the cellular response to stress at the G$_2$-M checkpoint. The growth arrest and DNA damage response gene *Gadd45a* appeared to be a direct target of FOXO3a that mediates part of FOXO3a's effects on DNA repair. These findings indicate that in mammals FOXO3a regulates the resistance of cells to stress by inducing DNA repair and thereby may also affect organismal life-span.

The binding of growth factors to specific receptor tyrosine kinases activates the phosphoinositide 3-kinase (PI3K) and the serine-threonine kinase Akt (also called protein kinase B or PKB). Akt promotes cell survival and proliferation in part by directly phosphorylating and inhibiting members of the FOXO subfamily of fork-head transcription factors (1–3). In the nematode *Caenorhabditis elegans*, null mutants of the PI3K-Akt pathway lead to the activation of the worm FOXO transcription factor DAF-16, resulting in either an extension of adult life-span or, during development, an entrance into the long-lived larval stage termed dauer (4, 5). In both cases, the PI3K-Akt pathway mutants develop a resistance to stress that may account for the longevity phenotype observed (4, 6). One possibility is that in the mutant background, the activation of FOXO transcription factors may mediate the resistance to stress because DAF-16's activity is required for the transcriptional up-regulation of cytosolic catalase and superoxide dismutase, scavenger proteins that protect against oxidative damage (7, 8). In mammals, the role of the forkhead transcription

[1]Division of Neuroscience, Children's Hospital and Department of Neurobiology, Harvard Medical School, Boston, MA 02115, USA. [2]Millennium Pharmaceuticals, Inc., 640 Memorial Drive, Cambridge, MA 02139, USA. [3]Building 37, Room 6144, NCI, National Institutes of Health, 37 Convent Drive MSC 4255, Bethesda, MD 20892, USA.

*These authors contributed equally to this work.
†To whom correspondence should be addressed. E-mail: michael.greenberg@tch.harvard.edu

factors in the response to stress is, as yet, unclear.

One mechanism by which cells protect themselves against oxidative stress is by repairing the damage to their DNA and proteins that occurs upon exposure to environmental stress (9). Furthermore, this capacity to repair DNA damage is closely correlated with an increased longevity in mammals (9). Therefore, we considered the possibility that the transcription factor FOXO3a, a mammalian forkhead family member that is similar in sequence to DAF-16, induces a program of gene expression that allows for the repair of DNA damage caused by oxidative stress. Under conditions of DNA damage, cycling cells arrest at one of two critical cell cycle checkpoints (G_1-S or G_2-M phase of the cell cycle, before and after DNA replication) allowing the cells time to repair their DNA (10).

Overexpression of FOXO3a induces a potent G_1 arrest (3), but FOXO3a's role in G_2-M progression has not been explored. Consistent with a possible role for FOXO3a in the G_2-M phase of the cell cycle, FOXO3a was localized in the nucleus in cells passing through the G_2 phase of the cell cycle [Web fig. 1 (11)]. To assess the role of FOXO3a in G_2-M progression, we generated a line of Rat-1 fibroblasts that express a fusion protein consisting of FOXO3a fused at its COOH terminus to the ligand-binding domain of the estrogen receptor (TM-ER) (11). In TM-ER, the FOXO3a moiety was mutated such that the key regulatory sites of phosphorylation, Thr[32], Ser[253], and Ser[315], were converted to alanine so that Akt could no longer phosphorylate these sites. The ER portion of this fusion protein was mutated so that it specifically responded to 4-hydroxytamoxifen (4OHT) but not to estrogen (12), thus rendering TM-ER refractory to activation by endogenous estrogen. In TM-ER, the ER domain functions as a molecular switch that rapidly turns on the activity of the FOXO3a protein when TM-ER expressing cells are exposed to 4OHT. Using antibodies that recognize the TM-ER protein, we found that in the absence of 4OHT, the TM-ER fusion protein was sequestered in the cytoplasm (Fig. 1A) (13). However, 1 hour after treatment of cells with 4OHT (1 μM), the TM-ER protein was found almost exclusively in the nucleus (Fig. 1A). We tested the ability of TM-ER to drive FOXO-dependent transcription in response to 4OHT. Activated TM-ER enhanced transcription of a luciferase reporter gene containing three canonical FOXO binding sites within its promoter [forkhead response element (FHRE) luciferase] (Fig. 1B). 4OHT did not induce the reporter gene in cells that did not express TM-ER (Fig. 1B), indicating

that the transactivation of the reporter was not a nonspecific effect of 4OHT treatment. 4OHT also did not induce FHRE luciferase expression in cells that expressed a mutant form of TM-ER that has a deletion in the DNA binding domain (TMΔDB-ER) (11) (Fig. 1B).

To examine the role of FOXO3a during progression from G_2 to M phase, we exposed Rat-1 cells stably expressing TM-ER to aphidicolin to arrest the cells in early S phase (11). The aphidicolin was then washed out to release the cells from the S phase block while FOXO3a activity was simultaneously induced by the addition of 4OHT. Fluorescence-activated cell sorting (FACS) analyses of the Rat-1 cells stably expressing the TM-ER at 7 hours after stimulation with 4OHT revealed a G_2-M delay (Fig. 2A). 4OHT alone did not affect the progression of control Rat-1 fibroblasts through the G_2 and M phases of the cell cycle (Fig. 2B). Importantly, FACS analyses of Rat-1 clones stably expressing TMΔDB-ER showed that treatment of cells with 4OHT no longer elicited a G_2-M delay, indicating that FOXO3a induces G_2-M delay by binding to DNA (Fig. 2B). The results obtained by FACS analyses were corroborated by immunocytochemistry experiments with the use of an antibody that specifically stains cells that are in the G_2 and M phases of the cell cycle [Web fig. 2, A and B (11)].

To verify that the G_2 delay observed in TM-ER–expressing clones also occurs in cells expressing endogenous FOXO3a, we treated Rat1 cells with the PI3K inhibitor LY294002 (LY), which promotes the translocation of endogenous FOXO3a to the nucleus (1, 14). We found that treatment of cells with LY also caused a delay in the passage of the cells though G_2 (Fig. 2C), further suggesting a role for FOXO3a in regulating G_2-M progression. It is possible that the delay in the progression through the G_2 phase induced by FOXO3a activation may allow time for the repair of damaged DNA before progression into M phase.

To determine if FOXO3a induces the repair of damaged DNA, we assessed FOXO3a's ability to reactivate an ultraviolet (UV)-damaged reporter gene in a host cell reactivation assay (15). We cotransfected a cytomegalovirus (CMV)-luciferase reporter plasmid that had been damaged before transfection by 5000 J/m² of UV irradiation together with various FOXO3a constructs and an undamaged CMV-renilla luciferase reporter control plasmid (11). The damaged reporter, unless repaired, does not display any transcriptional activity. FOXO3a does not substantially activate the CMV promoter (14). Any small tran-

scriptional effect of FOXO3a on the activation of the repaired CMV promoter is offset by normalization to the cotransfected undamaged CMV-renilla luciferase reporter gene that serves as an internal control. Expression of an active FOXO3a in both the RKO human colorectal cancer cell line and wild-type mouse embryonic fibroblasts (MEFs) promoted reactivation of the cotransfected UV-damaged CMV luciferase reporter (Fig. 3, A and B). The reactivation of the luciferase reporter gene by the constitutively active FOXO3a in both cell lines was significantly greater than the amount of reporter gene activation detected in the absence of FOXO3a ($P < 0.001$, t test). Moreover, a mutant of FOXO3a that has a deletion in FOXO3a DNA binding domain (TMΔDB) (11) was less effective at inducing the repair of the CMV promoter ($P < 0.001$ versus TM, t test) (Fig. 3A), indicating that FOXO3a induces DNA repair by binding to DNA, possibly to sites within the promoters of genes involved in the DNA repair process.

To confirm that FOXO3a induces the repair of damaged DNA, we used a quantitative polymerase chain reaction (PCR)-
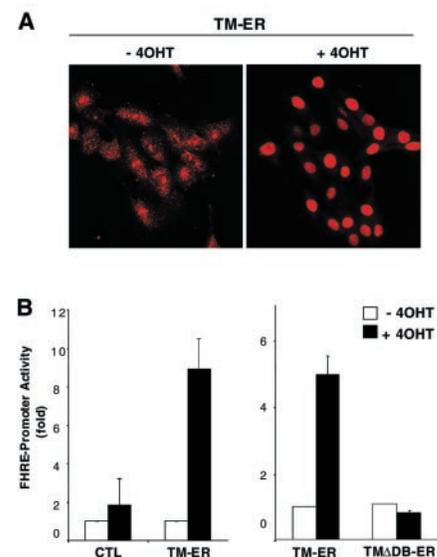

Fig. 1. Inducible activation of FOXO3a. (**A**) Rat1 cells expressing the inducible form of FOXO3a (TM-ER) were incubated in the presence (+) or absence (−) of 4OHT (1 μM) for 1 hour. The subcellular localization of TM-ER was monitored by immunofluorescence using the antibody to HA. (**B**) Control Rat 1 cells (CTL) and Rat 1 cells expressing TM-ER or TMΔDB-ER were transfected with the FHRE-luciferase reporter gene. One day after transfection, cells were incubated in the presence (+) or absence (−) of 1 μM 4OHT for 6 hours, and luciferase assays were performed. The graph represents the mean and SEM of three independent experiments conducted in duplicates.
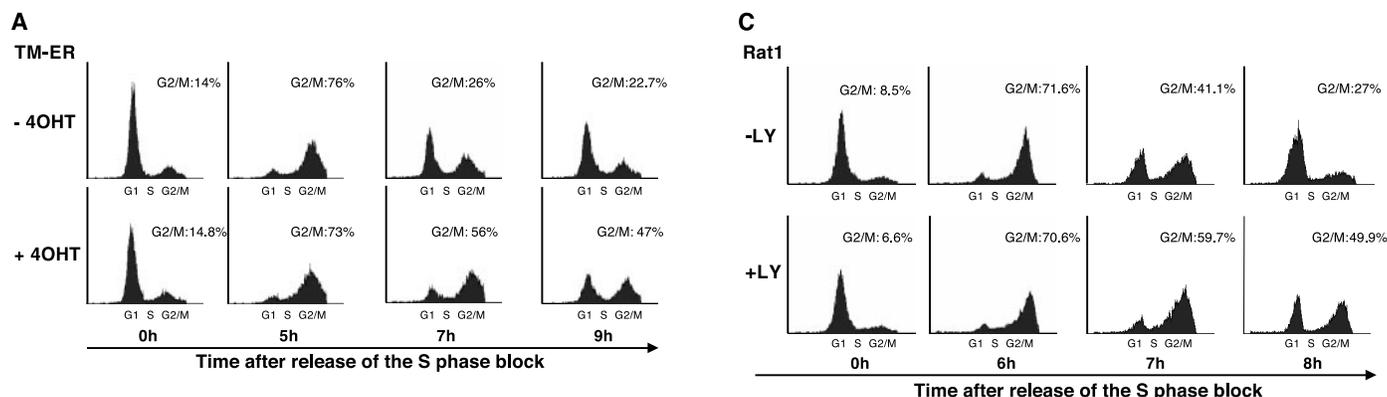
Fig. 2. FOXO3a induces a delay in G$_2$ to M progression. (**A**) Rat1 cells expressing TM-ER or TMΔDB-ER were released from an S phase block at various times in the presence or absence of 4OHT (500 nM). Fixed cells were stained with propidium iodide, and FACS analysis was performed. The percentage of cells in each phase of the cell cycle was calculated with CellQuest software (Becton Dickinson, San Jose, CA). The experiment presented is representative of four independent experiments. (**B**) Control Rat1 cells or Rat1 cells expressing TM-ER or TMΔDB-ER were released from an S phase block at 9 hours in the presence or absence of 4OHT (500 nM). FACS analysis was performed as described in (A). The data presented corresponds to the mean of two independent experiments. (**C**) Rat1 cells were released from an S phase block at various times in the presence or absence of LY (25μM). FACS analysis was performed as described in (A). The experiment presented is representative of two independent experiments.

based assay to detect the presence of damaged DNA templates that had been repaired (*11*). We cotransfected a DNA template damaged by 5000J/m^2 of UV irradiation together with various FOXO3a constructs and an undamaged control DNA template. Repair of the template was assessed by measuring its amplification by PCR and was quantified by real-time fluorescence detection. As with the promoter reactivation experiments, TM but not TMΔDB induced repair of the damaged template (Fig. 3C).

We used high-density cDNA microarrays to identify FOXO3a-regulated genes that might mediate the G$_2$-M delay and DNA repair response. We isolated messenger RNA (mRNA) from TM-ER–expressing Rat 1 cells at 0, 1, 3, and 8 hours after 4OHT addition and hybridized the mRNA to DNA microarrays containing 12,000 cDNAs and expressed sequence tags (ESTs) (*16*, *17*). Transcriptional profiles were compared, and a clustering algorithm was applied to identify genes regulated after FOXO3a activation. From this clustering analysis, we identified several genes involved in apoptosis and the regulation of the cell cycle (Table 1), consistent with the previously known functions ascribed to FOXO3a (*1*, *3*). FOXO3a also increased expression of a group of genes that takes part in the cellular response to stress. Expression of these genes was not increased in control Rat1 cells treated with 4OHT. Several of the genes expressed in response to activation of TM-ER also showed increased expression when cells were treated with the PI3K inhibitor LY (Table 1). Of
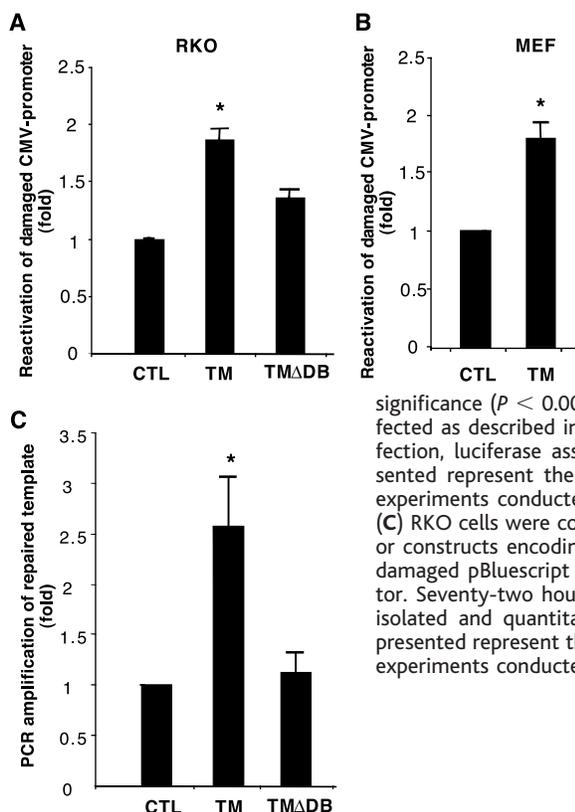

Fig. 3. FOXO3a-induced repair of damaged DNA. (**A**) RKO cells were cotransfected (Effectene, Qiagen, Valencia, CA) with 0.4 μg of empty vector or constructs encoding TM or TMΔDB, together with a UV-damaged CMV-luciferase reporter construct (0.5 μg) and an undamaged CMV-renilla luciferase reporter construct (0.1 μg). Twenty-four hours after transfection, luciferase assays were performed. The data presented represent the mean and SEM of five independent experiments conducted in duplicates. Asterisk indicates statistical significance ($P < 0.001$, *t* test). (**B**) WT MEFs were transfected as described in (A). Twenty-four hours after transfection, luciferase assays were performed. The data presented represent the mean and SEM of 10 independent experiments conducted in duplicates. ($P < 0.001$, *t* test). (**C**) RKO cells were cotransfected with empty vector (CTL) or constructs encoding TM or TMΔDB together with UV-damaged pBluescript and an undamaged pGL3-Basic vector. Seventy-two hours after transfection, total DNA was isolated and quantitative PCR was performed. The data presented represent the mean and SEM of six independent experiments conducted in triplicates.
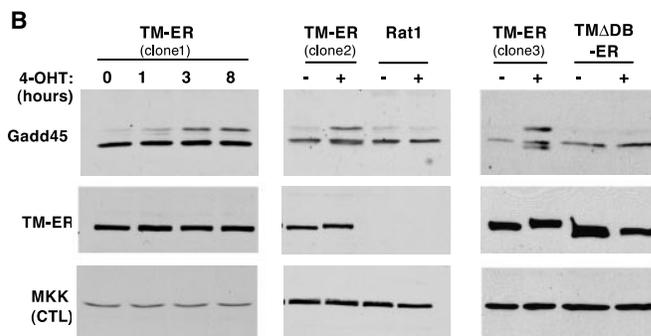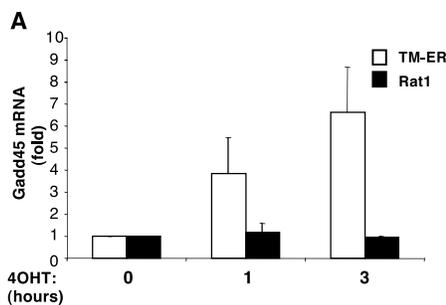
these genes, *Gadd45a* appeared to be a good candidate for mediating the effects of FOXO3a on G$_2$-M progression and DNA repair. All three members of the Gadd45 family, Gadd45a, Gadd45β, and Gadd45γ, are expressed in response to stress stimuli that induce DNA damage (*18–20*). The *GADD45A* promoter contains three FOXO

transcription factor binding sites (*21*). Of these sites, one is in a region that is conserved across species, suggesting that its function is critical. Lastly, Gadd45a is important for DNA repair and cell cycle arrest at the G$_2$-M checkpoint (*22–24*).

To verify that FOXO3a regulates Gadd45a expression, we isolated mRNA at

Fig. 4. FOXO3a-induced expression of Gadd45a mRNA and protein. (**A**) Rat1 cells either expressing empty vector (solid bars) or TM-ER (open bars) were stimulated with 4OHT (1 μM) for 0, 1, and 3 hours. Real-time quantitative RT-PCR was performed with the use of primers to Gadd45a cDNA. (**B**) (Left) Rat1 cells expressing TM-ER were stimulated with 4OHT (1 μM) for 0, 1, 3, or 8 hours. Western blot experiments were performed with the antibody to Gadd45a (top), the antibody to HA to detect TM-ER (middle) and an antibody to a control protein (MKK1) to monitor equal loading (bottom). (Center) A clone of Rat1 cells expressing TM-ER and the control Rat1 cells were incubated in the presence (+) or absence (–) of 4OHT (1 μM) for 8 hours. Western blot experiments were conducted as described above. (Right) Clones of Rat 1 cells expressing TM-ER or TMΔDB-ER were incubated in the presence (+) or absence (–) of 4OHT (1 μM) for 8 hours. Western blot experiments were conducted as described above.
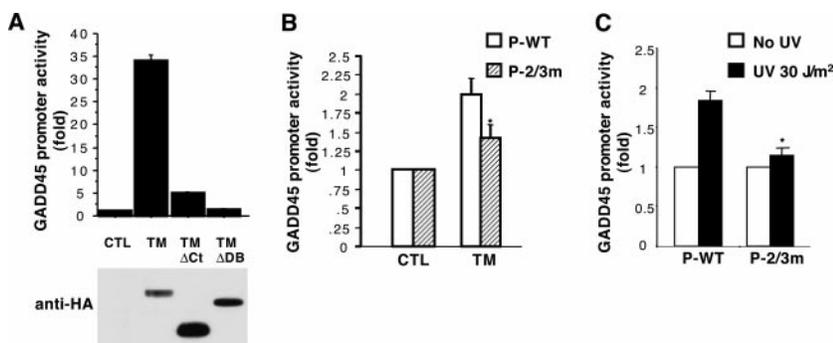

Fig. 5. Expression from the *GADD45A* promoter induced by FOXO3a through direct binding to two FHREs. (**A**) CCL39 cells were cotransfected with empty vector (CTL) or constructs encoding TM, TM-ΔCt, or TM-ΔDB together with the *GADD45A*-luciferase reporter plasmid. Thirty-six hours after transfection, luciferase assays were performed. (**B**) CCL39 cells were cotransfected with CTL or with a construct encoding TM together with the wild-type *GADD45A* luciferase reporter construct (P-WT, open bars) or the double mutant *GADD45A* luciferase reporter construct (P-2/3m, hatched bars). Twenty-four hours after transfection, luciferase assays were performed. Asterisk indicates statistical difference from P-WT cotransfected with TM ($P <$ 0.05, t-test). (**C**) CCL39 cells were transfected with either P-WT or P-2/3m. The cells were then either treated (solid bars) or not treated (open bars) with 30 J/m² of UV irradiation for 6 hours, and luciferase assays were performed ($P <$ 0.005, t test).

hour 0, 1 hour, and 3 hours after exposure of TM-ER–expressing cells to 4OHT. By real-time quantitative reverse transcriptase–PCR (RT-PCR), we found that expression of the Gadd45a mRNA was induced upon exposure of TM-ER–expressing cells to 4OHT (Fig. 4A) (*11*). Western analysis with a Gadd45 antibody revealed that the abundance of Gadd45a protein increased in three independent TM-ER–expressing clones in response to 4OHT treatment (Fig. 4B) (*13*). In contrast, 4OHT did not increase abundance of Gadd45a mRNA or protein in cells that did not express the TM-ER protein (Fig. 4, A and B), nor did 4OHT cause accumulation of the Gadd45a protein in cells that expressed TMΔDB-ER (Fig. 4B).

To determine if the induction of Gadd45a transcription is mediated by the direct binding of FOXO3a to the promoter of the *Gadd45a* gene, we examined the effects of FOXO3a on the activity of the human *GADD45A* promoter. An analysis of the human *GADD45A* promoter revealed the presence of one conserved consensus FHRE, ATAAACAA, at 505 nucleotides 5′ of the transcriptional start site, and two suboptimal FHREs, TAAAACAA and TTGTTTGG, located 377 and 803 nucleotides 5′ of the transcriptional start site, respectively. To assess the ability of FOXO3a to regulate *GADD45A* transcription, we cotransfected CCL39 fibroblast cells with various FOXO3a constructs together with a reporter gene in which the *GADD45A* promoter drives the expression of a luciferase gene (*13*). We found that the constitutively active mutant of FOXO3a (TM) but not a mutant in which the transactivation domain was deleted (TMΔCt) effectively induced *GADD45A* promoter driven luciferase activity (Fig. 5A). A mutant of FOXO3a that does not bind DNA

(TMΔDB) did not activate *GADD45A* promoter expression (Fig. 5A).

GADD45A promoters in which we replaced the core consensus sequence AACA of FHRE-2 within the *GADD45A* promoter with GGGG and also replaced the AC within the core consensus sequence of FHRE-3 with GG (P-2/3m) showed diminished activity in response to FOXO3a ($P <$ 0.05, t test) (Fig. 5B). Thus, direct DNA binding of FOXO3a to FHRE-2 and FHRE-3 of the *GADD45A* promoter appears to be important for the transactivation of the *GADD45A* promoter.

To determine if FOXO3a promotes UV expression of Gadd45a in cells exposed to UV irradiation, we transfected CCL39 fibroblasts with a luciferase reporter containing either the wild-type *GADD45A* promoter or the double mutant *GADD45A* promoter construct (P-2/3m) and exposed the cells to 30J/m² of UV irradiation. The UV responsiveness of the *GADD45A* promoter was diminished when the FOXO3a binding sites were mutated ($P <$ 0.005, t test) (Fig. 5C), suggesting that FOXO3a mediates the UV induction of the *GADD45A* promoter.

We used *Gadd45a*-deficient fibroblasts to determine whether FOXO3a's ability to induce a G₂ delay and DNA repair requires the activity of Gadd45a. We assessed the G_2 progression of wild-type (WT) or *Gadd45a*$^{-/-}$ fibroblasts by FACS analysis in the absence or presence of the PI3K inhibitor LY, which activates endogenous FOXO3a. The LY-induced G_2 delay was somewhat diminished in the *Gadd45a*$^{-/-}$ fibroblasts compared with that in WT (Fig. 6A), suggesting that Gadd45a may be partly required for the G_2 delay induced by the activation of endogenous FOXO3a. We note that in the absence of LY, the *Gadd45a*$^{-/-}$ fibroblasts exhibit a slowed progression through the cell cycle compared with the WT fibroblasts (Fig. 6A), presumably due to the accumu-

Fig. 6. FOXO3a-induced G_2-M delay and DNA repair is mediated by Gadd45a. (**A**) Transformed WT MEFs or $Gadd45a^{-/-}$ fibroblasts cells were released from an S phase block at hour 0 or 9 hours in the presence or absence of LY (25μM). FACS analysis was performed as described in Fig. 2C. The experiment presented is representative of two independent experiments. (**B**) $Gadd45a^{-/-}$ MEFs (solid bars) and WT MEFs (open bars) were transfected as described in Fig. 5A. Twenty-four hours after transfection, luciferase assays were performed. The data presented represent the mean and SEM of six independent experiments. Asterisk indicates statistical difference from $Gadd45a^{-/-}$ MEF transfected with TM ($P < 0.05$, two-sample t test).
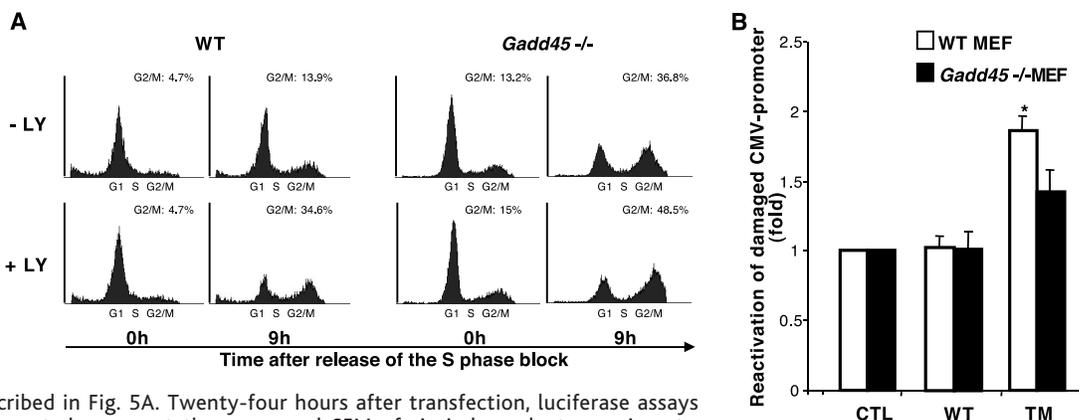

Table 1. Identification of FOXO3a target genes by transcriptional profiling.

Genes	Function	Microarray		Northern	FHRE
		FOXO3a	LY	FOXO3a	
DNA repair					
GADD45 and PA26	Growth arrest and DNA damage	2.1	1.4	2.3	+
	response	2.0	2.9	3.6	+
Antioxidant					
Selenoprotein P		2.3	1.0	5.3	+
Cell cycle					
Wip1	Phosphatase	2.2	1.7	ND	+
EXT1	Tumor suppressor	2.0	1.0	ND	+
Cyclin G2	G2-delay	1.3	2.2	ND	+
Cell death					
Legumain	Cysteine protease	1.6	1.7	ND	+
NIP3	Pro-apoptotic	1.4	1.5	ND	ND
	Bcl-2 family member				

lation of cells in S phase, as had been observed previously (*22*). The effect of FOXO3a TM on reactivation of the damaged CMV reporter gene was diminished in the $Gadd45a^{-/-}$ MEFs compared with the WT MEFs ($P < 0.05$, two-sample t test) (Fig. 6B), indicating that Gadd45a mediates, at least in part, FOXO3a-dependent DNA repair.

These findings define a role for FOXO3a in inducing a delay in the G_2-M phase in response to stress stimuli during which FOXO3a contributes to the repair of damaged DNA by a Gadd45a-dependent mechanism. FOXO3a can also induce cell cycle arrest in G_1 (*3*) and can enhance the exit from M phase (*25*), suggesting that FOXO3a has multiple roles in cell cycle control. FOXO3a's ability to induce G_1 arrest, apoptosis, and, as we show here, G_2-M delay and DNA repair, makes it an attractive candidate as a tumor suppressor in a manner reminiscent of the tumor suppressor protein p53. Loss of FOXO3a function may lead to a decreased ability to induce cell cycle arrest at the critical G_1-S and G_2-M checkpoints, leading to tumor development.

Our findings suggest that an important role for the forkhead transcription factors in stress-resistance and the aging process may be conserved in mammals. An organism's ability to respond to stress, in particular the capacity of cells to repair damage to DNA, correlates with an increased longevity (*26*). We propose that under low stress conditions, FOXO3a may promote DNA repair, whereas under higher levels of stress, FOXO3a may induce a program of cell death. This graded response to stress stimuli would protect cells from damage but also facilitate the removal of heavily damaged cells, resulting in an overall increase in the life-span of the organism.

References and Notes
1. A. Brunet *et al.*, *Cell* **96**, 857 (1999).
2. G. J. Kops *et al.*, *Nature* **398**, 630 (1999).
3. R. H. Medema, G. J. Kops, J. L. Bos, B. M. Burgering, *Nature* **404**, 782 (2000).
4. S. Ogg, *et al.*, *Nature* **389**, 994 (1997).
5. K. Lin, J. B. Dorman, A. Rodan, C. Kenyon, *Science* **278**, 1319 (1997).
6. P. L. Larsen, *Proc. Natl. Acad. Sci. U.S.A.* **90**, 8905 (1993).
7. J. Taub *et al.*, *Nature* **399**, 162 (1999).
8. Y. Honda, S. Honda, *Faseb J.* **13**, 1385 (1999).
9. T. B. L. Kirkwood, S. N. Austad, *Nature* **408**, 233 (2000).
10. B. B. Zhou, S. J. Elledge, *Nature* **408**, 433 (2000).
11. Supplementary Web material is available on *Science* Online at www.sciencemag.org/cgi/content/full/296/5567/530/DC1.
12. T. D. Littlewood, D. C. Hancock, P. S. Danielian, M. G. Parker, G. I. Evan, *Nucleic Acids Res.* **23**, 1686 (1995).
13. Western blot, immunofluorescence experiments, and luciferase assays were performed as described (*1*). The $GADD45\alpha$ (H-165) antibody was purchased from Santa Cruz.
14. A. Brunet, H. Tran, M. E. Greenberg, unpublished data.
15. M. L. Smith *et al.*, *Oncogene* **13**, 2255 (1996).
16. L. W. Chiang *et al.*, *Proc. Natl. Acad. Sci. U.S.A.* **98**, 2814 (2001).
17. Isolation of mRNA and transcriptional profiling experiments were performed as described previously in (*16*) and as decribed in (*11*).
18. A. J. Fornace Jr. *et al.*, *Mol. Cell. Biol.* **9**, 4196 (1989).
19. M. Takekawa, H. Saito, *Cell* **95**, 521 (1998).
20. Q. Zhan *et al.*, *Mol. Cell. Biol.* **13**, 4242 (1993).
21. The plasmid encoding the *GADD45A* promoter driving the luciferase reporter gene and HA-*GADD45A* in a mammalian expression vector were kind gifts of D. Haber and were described previously (*27*).
22. M. L. Smith *et al.*, *Mol. Cell. Biol.* **20**, 3705 (2000).
23. X. W. Wang *et al.*, *Proc. Natl. Acad. Sci. U.S.A.* **96**, 3706 (1999).
24. M. C. Hollander *et al.*, *Nature Genet.* **23**, 176 (1999).
25. B. Alvarez, A. C. Martinez, B. M. Burgering, A. C. Carrera, *Nature* **413**, 744 (2001).
26. T. B. Kirkwood, *Mutat. Res.* **219**, 1 (1989).
27. D. P. Harkin *et al.*, *Cell* **97**, 575 (1999).
28. We thank members of the Greenberg lab for their support. In particular, we thank A. Nigh and W. Chen for help with the quantitative real-time PCR; A. West, J. Zieg, and R. Dolmetsch for their comments on the manuscript; B. Demple for helpful discussions and critical reading of manuscript; and A. Flint for his help in analyzing the FACS samples at the Howard Hughes FACS Facility. Supported by a Senior Scholars Award from the Ellison Foundation, NIH grant PO1-HD24926, and Mental Retardation Research Center grant, NIHP30-HD18655 (M.E.G.). A.B. was supported by a Goldenson Berenberg Fellowship. M.E.G. also acknowledges the generous contribution of the F. M. Kirby Foundation to the Division of Neuroscience.

5 December 2001; accepted 12 March 2002